Molecular Dynamics Simulation of Dextran Extension at Constant Pulling Speed

Igor Neelov,[1,2,3] *David Adolf,*[2] *Marina Ratner,*[4] *Oleg Zhicol,*[5] *Tom McLeish*[2]

Summary: A dextran monomer and a 10mer under constant pulling speed were studied using the atomistic simulations. Molecular dynamics (MD) with the new Amber-Glycam04 forcefield were performed. The main result of the present Amber-based MD simulations is that the experimental plateau of the force-extension dependence for dextran can be explained by a transition of the glucopyranose rings in the dextran monomers from a chair ($^4C_1$) to a inverted chair ($^1C_4$) conformation whereas chair to boat transitions occur at higher forces. Density functional (DFT) calculations of monomer were also performed for a monomer at different fixed end-to-end distances (lengths) to clarify the molecular mechanism of dextran extension. These DFT calculations confirm the existence of an inverted chair ($^1C_4$) conformation at intermediate extensions and its possible important contribution to the plateau in the experimental force-extension dependence of dextran.

Keywords: dextran; extension; polysaccharides; simulation; single molecule AFM

Introduction

Polysaccharides are fundamental components of cells and have many potential applications in the pharmaceutical industry and material science. Mechanical properties of polysaccharides are important because they constitute cell walls in plants and bacteria and take part in cell interactions and adhesion. They also serve as a simple model for studies into the mechanical properties of protein concatemers. Dextran is an important representative of polysacchrides with 1-6 linkages (i.e. connecting C_1 and C_6 carbon atoms on neighbouring sugar monomers). The mechanical extension of dextran has been performed in single molecule AFM experiments by Rief et al.[1] and by Marszalec et al.[2] A key finding was the existence of a plateau in the force-extension dependence for dextran at forces near 700–1000 pN. Additionally Rief et al. performed molecular dynamic (MD) simulations of dextran 5mer extension at a constant pulling speed of 0.25 Å/ps to obtain the force-extension curve. Rief et al. attributed the plateau to a rotation around C_5–C_6 bonds (i.e. to conformational transition of $O_5C_5C_6O_6$ angle) while Marszalec and Fernandes suggested the plateau occurs due to a forced chair-boat transition of the glucopyranose rings.

Recently, Lee et al.[3] presented results of a MD simulation of dextran extension at constant pulling speed. A CHARMM based force field elaborated by Kuttel et al.[4] was used. With this forcefield it was observed that the glucopyranose ring conformational transition from the chair to the boat conformation is the main source of the plateau on the force-extension curve.

In our recent work[5] Amber-based (Amber94 and Amber Glycam04) forcefields were used to study the extension of

[1] Institute of Macromolecular Compounds, RAS, Bolshoi pr. 31, 199004, St. Petersburg, Russia, neelov@imc.macro.ru
[2] IRC in Polymer Science and Technology, University of Leeds, Leeds LS2 9JT, UK, E-mail: phyin@phys-irc.leeds. ac.uk
[3] Laboratory of Polymer Chemistry, PB55, University of Helsinki, Finland
[4] Institute for Single Crystals, NASU, 60 Lenin Avenue, Kharkhov, Ukraine
[5] Institute of Scintillation Materials, NASU, 60 Lenin Avenue, Kharkhov, Ukraine

© 2006 WILEY-VCH Verlag GmbH & Co. KGaA, Weinheim

dextran and its monomer at different constant forces. In addition to Lee and Marszalec chair-boat transitions, a significant amount of forced transitions from the chair ($^4C_1$) to inverted chair ($^1C_4$) conformation was found in the plateau region. In the present paper, we study the extension of dextran at constant pulling speed as in the work of Lee et al. but employ an Amber-like forcefield. Density functional (DFT) calculations of the dextran monomer at different fixed lengths were also performed.

Models and Methods of Molecular Simulation

Amber[6], CHARMM[7] and some other forcefields (for example, MM3[8]) and their modifications (united atom Amber[9], Amber-Homans[10], Amber-Glycam[11], Amber with GB/SA continuum model of water[12], CHARMM-Parm22/SU01[13]) have been used for the simulations of monosaccharides.

A comparison of 20 different forcefields for monosaccharides was carried out recently.[14] The largest deviation from density functional results was observed for CHARMM22, Gromos, MM3* and some other forcefields. Surprisingly the best forcefield in this review was found to be the Amber-like forcefield (Amber94) which was not specially designed for carbohydrates.

In cited paper of Lee et al., it was shown that solvent has no significant effect on the force-extension behaviour of dextran. They also evaluated characteristic conformational transition times in dextran between 10^{-9} s and 10^{-6} s. The only way to achieve this interval of times in molecular dynamics simulation is to perform MD without an explicit solvent. These reasons explain the absence of water molecules in most of their and our simulations.

In this paper, the results of MD simulations of the extension of the dextran monomer and 10mer at constant puling speed are presented. The C6–O6 bonds in the dextran were initially distributed between their gt and gg states in accordance with experimental data (gt/gg/tg = 40:60:0). End-to-end vector of was oriented initially along the extension axis (i.e. axis X). The most recent version (Amber-Glycam04) of the Amber-Glycam forcefield was used. One chain end was fixed and the other (pulled) end was restrained harmonically to another point which was moved with constant speed dx/dt (dx/dt = 0.1–0.00001 Å/ps) along the X axis. Several elasticity constants were used for this restraining from the interval 50–1000 pN/nm to resemble the usual elasticity of cantilevers. The Verlet algorithm with a time step $\Delta t = 1$ fs was used in all simulations. To achieve suitable local equilibration of dextran without explicit solvent molecules, the Andersen thermostat[15] was used.

In addition to MD simulation, we performed density functional (DFT) calculations of the energies and the conformations of the dextran monomer at different monomer lengths *d* (distances between O1 and O6 atoms) from d = 4.4 Å to d = 6.5 Å. Electronic structure calculations were carried out by three methods. Firstly, with the DFT B3LYP/6-31G** method (functional includes Becke 3-parameter exchange and Lee-Yang-Parr correlation; Pople double-zeta basis set with polarization fucntions used) equilibrium configurations and potential curves for molecule stretching were obtained. Secondly, the equilibrium configurations were optimized with the B3LYP/aug-cc-pVTZ method (Dunning correlation consistent basis set containing several diffuse and polarization shells per atom). Finally, several single point MP2 (second order Møller-Plesset perturbation theory) calculations for the best obtained equilibrium configuration geometries were performed: with the MP2/aug-cc-pVTZ// B3LYP/aug-cc-pVTZ method. Combination of the B3LYP functional with a 6-31G** basis set usually provides good results for the geometry and the energies of molecules without an extended conjugated π-system. At the same time it is well-known that this method slightly overestimates the strength of hydrogen bonds. The change of the basis set to a much more

© 2006 WILEY-VCH Verlag GmbH & Co. KGaA, Weinheim

extended aug-cc-pVTZ leads to an increase of the hydrogen bond lengths, but does not change the relative energy. Calculations were carried out using GAMESS US and GAUSSIAN98.

Results and Discussion

Extension of 10mer and Monomer

The extension of a dextran 10mer was simulated at constant pulling speeds 0.1–0.0001 Å/ps. The pulling speed in single molecule AFM experiments is usually several order of magnitude lower so the most of figures in this paper will be shown for the slowest speed used. Force-extension curve (i.e. force F acting on the pulled chain end in the direction of extension, as function of the extension is presented in Fig. 1a. In pulling experiments this dependence is qualitatively very similar with time dependence (because pulling speed is constant) but gives additional information about length of chain at which conformational transitions occurs. There are rather strong thermal fluctuations of the force at room temperature. At small and high extensions the force depends linearly on extension and the ratio of the elasticity constants for these regions is nearly 1:3 which is in agreement with the experimental data. At the intermediate extensions (between 54 and 58 Å) there is a clear plateau on this curve. The value of the plateau force between 800–900 pN is in agreement with the experimental plateau force (700–1000 pN) for dextran. At small and high extensions a similar dependence for zero temperature (gray dashed line in Fig. 1a) is very close (but without thermal fluctuations) to that at T = 300 K. But due to lack of thermal fluctuations the plateau region at zero temperature appears at higher extensions (59–60 Å and at forces more than twice higher (near 2000 pN).

It is necessary to take into account that the end-to-end distance of the 10mer is less than the sum of the monomer length (contour length) since the monomers are not perfectly orientated along the axis of extension. Thus the evaluation of monomer length from a normalized end-to-end distance leads to an underestimation of this value especially at small extensions. To find the real average monomer length we calculate the contour length of the chain and plot its dependence on force in Fig. 1a both at T = 300 K (line 3) and at T = 0 K (line 4). At high distances the extension (lines 1 and 2) and the contour length (lines 3 and 4) dependencies for each temperature coincide but at small distances dependencies on contour length drop abruptly at d near 52 Å (i.e. at average monomer length 5.2 Å) in comparison with force-extension curves. The plateau region (55–58 Å) for force-contour length dependence is also shorter and displaced to slightly higher distances than for force-extension curves.

To understand the molecular mechanisms of the dextran extension it is necessary to see the behaviour of monomers under extension. There are two ways of of doing this. First, to see the extension behaviour of each monomer in the 10mer under extension. Second to perform an additional simulation of a single dextran monomer extension at constant pulling speed. We applied both these approaches in the present paper. Fig. 1b gives the dependence of length of each monomer (distance between O1–O6 atoms) in 10 mer as a function of the extension of chain as whole. It is easy to see that until d = 5.4 Å only small linear extension of the monomers occurs. In the interval d = 5.4 Å–5.8 Å, a step-like increase of monomer length occurs for almost all monomers. Subsequently, a second interval of step-like increases in monomer lengths can be seen at d = 6.0–6.3 Å.

The force-extension curve for a single dextran monomer extended with constant pulling speed 0.00001 Å is presented in Fig. 1c for T = 300 K (solid line) and T = 0 K (dashed line). It is easy to see that it also reflects three different stages of extension at room temperature. In the first stage (end-to-end distance d between 5,3 Å and 5.8 Å) there is almost a linear dependence of force on extension (constant elasticity). In the

© 2006 WILEY-VCH Verlag GmbH & Co. KGaA, Weinheim

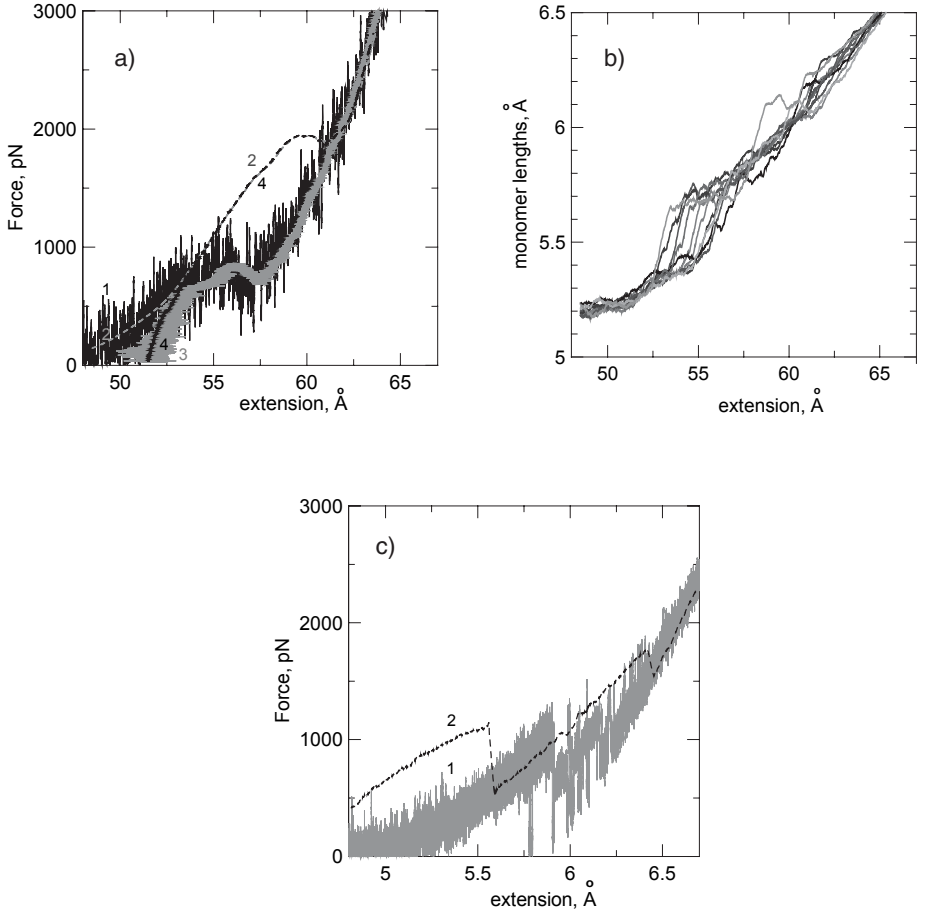

Figure 1.
a) Force-extension dependence for dextran 10mer extended at constant pulling speed 0.0001 Å/ps (solid lines 1 at T = 300 K, and 2 at T = 0 K), and force vs contour length (dashed lines 3 and 4, correspondingly) b) Monomer length for each of 10 monomers as function of extension at T = 300 K, c) Force-extension dependence for single monomer extended at T = 300 K (1) and T = 0 K (2).

interval d = 5.8 Å–6.2 Å the two step-like drops of force (at near 5.8 and 6.2 Å) can be clearly seen which divide the second stage of extension from the first and the third stages. Between d = 5.6 Å–6.2 Å the monomer has three different slopes of linear force-extension dependencies: initial (with small slope and higher forces), second intermediate slope (with intermediate forces) and third highest (with lowest forces). This reflects three different conformation states of the monomer. The first state dominates at d = 5.6 Å–5.8 Å (and lower extensions), the second state – at d = 5.8 Å–6.2 Å while the third state become dominant at higher extensions. At high distances, the slope of the force-extension dependence (elasticity constant) is nearly 3 times higher than at small distances(at d < 5.6 Å).

To understand the molecular mechanism of the dextran extension, we need to take into account that the monomer length can be increased by rotation around C5–C6 bond attached to monomer glucopyranose ring (the mechanism of dextran extension suggested by Ries et al.) or by conformational transition of ring itself (for example due to chair-boat transitions suggested by Marszalec et al. and observed in

© 2006 WILEY-VCH Verlag GmbH & Co. KGaA, Weinheim

CHARMM based MD simulations by Lee et al.). Thus we need to check contributions of both mechanisms separately.

The orientation of the C5C6 bond is defined by the conformation of two dihedral angles O5C5C6O6 and C4C5C6O6. Fig. 2a and 2b show the behaviour of these dihedral angles (O5C5C6O6 in Fig. 2a) and ($C_4C_5C_6O_6$ in Fig. 2b) for dextran 10mer during extension. Each plot contains the values of the angles for each of the 8 monomers (excluding two end monomers). For unperturbed monomer the dominant conformations of C5C6 bonds should be g+ (gauche+, 60°) for the first angle and t (trans, 180°) for the second one (i.e. g + t conformation of C5C6 bond with monomer length 4.5 Å and g-g+ (i.e. −60° or g- for first type of angles and 60° or g+ for second angles) with monomer length 5.2 Å. But it is easy to see from Fig. 2a and 2b that already at small extension of the 10mer the dominant conformation of C5C6 bond is g-g+ conformation. At these extensions some amount of tg- (180°, 60°) conformation and a very small number of g + t conformation are also present. This result is in agreement with results of Lee et al.

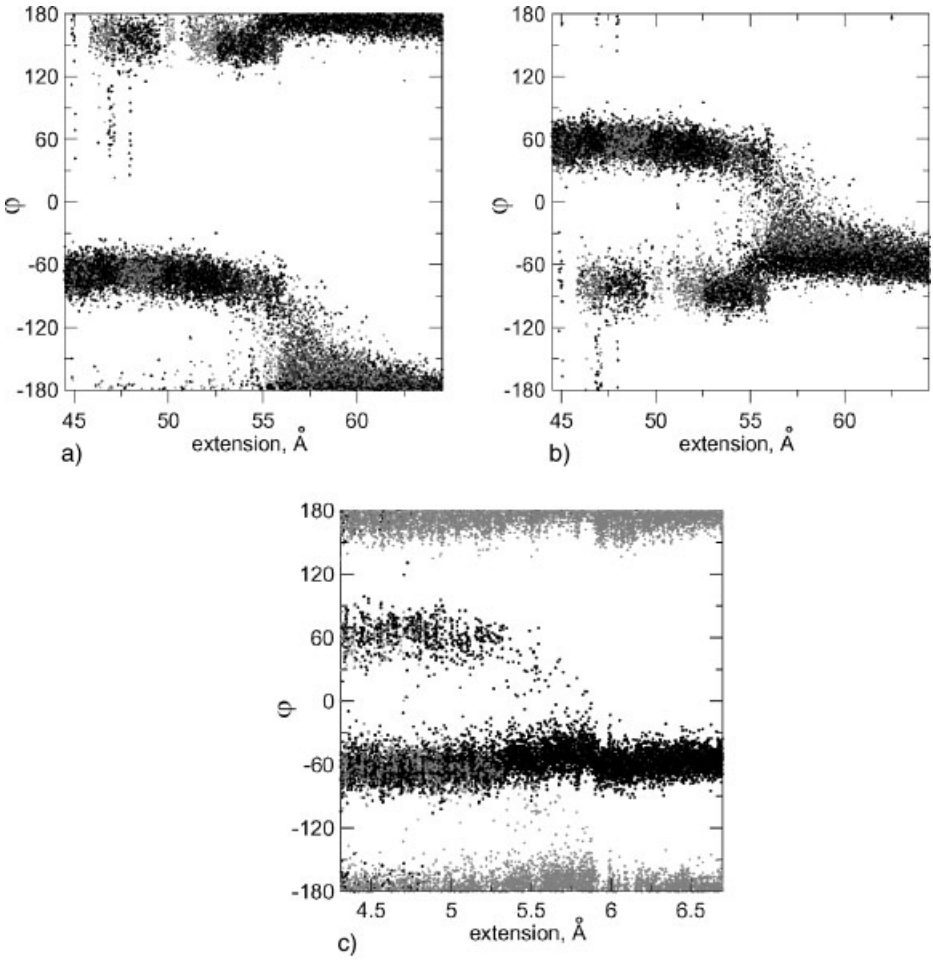

Figure 2.
Dihedral angles a) O5C5C6O6 and b) C4C5C6O6 for the 10mer (the angles for each of 8 monomer (excluding end monomers) are drown by different gray to black colours) and c) both of these angles for the monomer (O5C5C6O6 (gray) and C4C5C6O6 (black)) as function of extension.

© 2006 WILEY-VCH Verlag GmbH & Co. KGaA, Weinheim

(2004) that at room temperature at very early stage of extension, the transition from gt state of C6–O6 bonds with short monomer length d = 4.5 Å to gg states with longer monomer length d = 5.2 Å occur. After the extension of 10mer to 55–57 Å the transitions from of g-g+ (−60°,60°) to tg- (180,−60°) conformational state occur. But these transitions shouldn't change the length of the monomer and the 10mer because both g-g+ and tg- conformations have near the same monomer length. Thus the origin of plateau in force-extension dependence at room temperature is probably the transition of glucopyranose rings in each of dextran monomers.

To check the molecular structure of the glucopyranose rings (chairs, boats etc) it is possible to calculate some improper dihedral angles. Similar information can be obtained, for example, from the dihedral angles C2C1O5C5 (Fig. 3a) and C2C3C4C5 (Fig. 3b) as function of extension. Each plot contains corresponding angles for each 8 non-end monomers of the 10 monomers. If the first type of the angles is close to −60°, and the second is roughly +60° it corresponds to the unperturbed chair ($^4C_1$) conformation of glucopyranose ring which should be dominant in the absence of extension. If these angles have reverse signs (+60°, −60°) it corresponds to an inverted chair ($^1C_4$) conformation. If both angles have the same sign (both positive or both negative) it corresponds to the boat-like states of the glucopyranose ring. At small extension (between 45 and 56 Å) all angles of the first type (Fig. 3a) fluctuate around −60° and angles of the second type (Fig. 3b) – around 60°. It means that all rings in the 10mer are initially in the unperturbed chair ($^4C_1$) conformation. At distances near 56 Å the significant amount of the positive values of first type of angles in Fig. 3a plot and the negative values in Fig. 3b plot occur. If these angles switch sign simultaneously in the same monomer it means that the transition of the ring from chair ($^4C_1$) to inverted chair ($^1C_4$) occurs. It is the case for at least some monomers in Fig. 3a and 3b (see for example light grey points between extension 58 and 62 Å on Fig. 3a and 3b, corresponding to extension of 6th monomer). But some monomers did not change signs of these two dihedral angles (i.e. stay in $^4C_1$ conformation) while some others change sign of only first angle (Fig. 3a). In last case we have a transition to the boat state. This boat state (both angles are positive) becomes dominant at the extensions of the 10mer greater than 62 Å. The large fluctuations of the dihedral angles at these highest distances are probably due to the coexistence of boat and twisted boat conformations. A similar but more clear picture can be seen from the same plot for the single dextran monomer (Fig. 3c). Because for the monomer we have only one angle of each type (C2C1O5C5 (gray) and C2C3C4C5 (black) it is easy to see that they change sign in transition region (5.8–6.2 Å) simultaneously. It means that we have significant amount of the inverted chair conformation $^1C_4$ (the first angle is positive and the second is negative) in the region where force-extension dependence has plateau (see Fig. 1a and Fig. 1c). Due to thermal fluctuations there are also some part of the initial chair $^4C_1$ state (the first angle is negative and the second angle is positive) and the boat state (both angles have the same positive sign) in this region. Thus in the transition region there is coexistence of all three states (chair, inverted chair and boat). And it is easy to see from Fig. 3c that the boat (both angles positive) become a dominant state at higher extensions.

DFT Calculations for Monomer

Several lowest energy conformations of α-glucopyranose monomer selected from the molecular dynamics simulation, were studied. These conformations present two types of chairs ($^4C_1$ and $^1C_4$) and several boat and twisted boat conformations. For each conformation of the glucopyranose ring the three possible sub-states obtained by rotation around C5–C6 bond (pairs of dihedral angles O5C5C6O6 and C4C5C6O6 known as gt, gg and tg states) were probed.

© 2006 WILEY-VCH Verlag GmbH & Co. KGaA, Weinheim

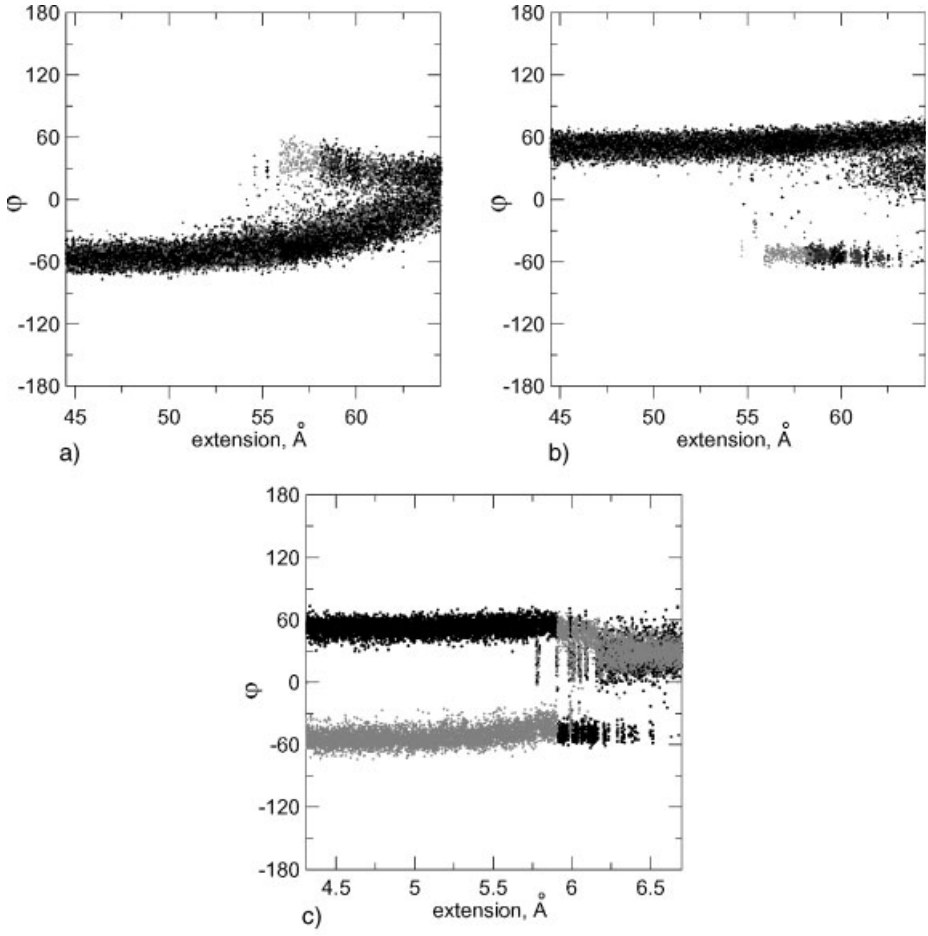

Figure 3.
Dihedral angles a) C2C1O5C5 and b) C2C3C4C5 for the 10mer (the angles for each of 8 monomer (excluding the end monomers) are drown by different gray to black colours), c) Angles (C2C1O5C5 (gray), C2C3C4C5 (black)) for monomer vs extension.

All these conformations were minimized and the geometrical paramenters including dihedral angles were calculated. It was obtained that the relative energies and the geometrical parameters of the most stable conformations are in good agreement with results of Apfel et al. (2004). These conformations were used as initial conformation for calculations of energy and geometry of the monomer at different fixed monomer lengths (distances between O1 and O6 atoms) from $d_0 = 4.4$ Å to $d_{max} =$ 6.5 Å. The fixed monomer length was increased at each step by $\Delta d = 0.1$ Å and full minimization was done as described above at each value of $d = d_0 + k\Delta d$ Dd ($k = 1,21$).

Fig. 4a shows the dependence of the energy on monomer length for different initial conformations of the dextran monomer. At small monomer length $d < 4.8$ Å the most favourable conformation of glucopyranose ring is chair $^4C_1$ with gt conformational state of C5–C6 bond (filled circles). This conformation has minimum energy at $d = 4.4$–4.5 Å close to zero and is the most favourable conformation of monomer in this region. Its energy increases with the distance d at all $d >$ 4.5 Å while for other two sub-states of chair

© 2006 WILEY-VCH Verlag GmbH & Co. KGaA, Weinheim

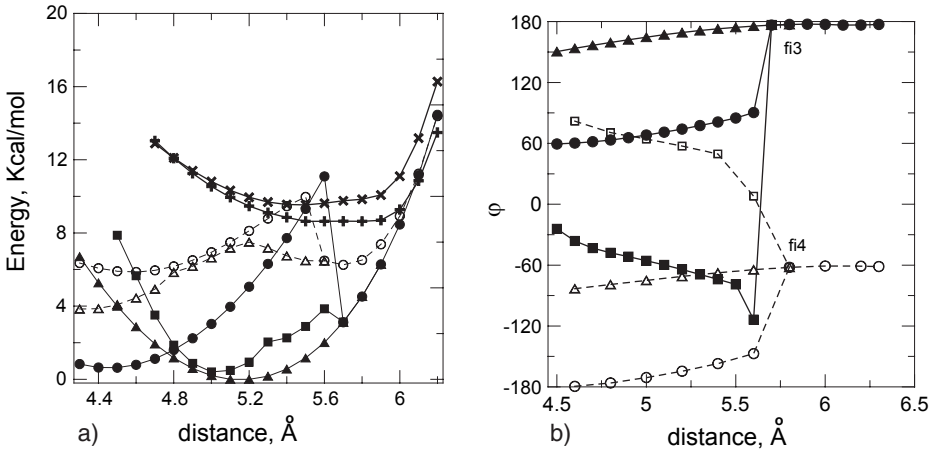

Figure 4.
a) Energy of different conformation states of dextran monomer. Chair $^4C_1$: g + t (filled circles), g-g+ (filled squares), tg- (filled triangles). Inverted chair $^1C_4$ (open circles and triangles). Boat and twisted boat conformations (x-symbols an crosses, correspondingly); b) dihedral angles fi3 = O5C5C6O6 (solid lines and filled symbols) and fi4 = C4C5C6O6 (dashed lines and open symbols) as function of fixed distance (g + t conformation (circles), g-g+ conformation (squares) and tg- conformation (triangles)).

$^4C_1$ (with gg and tg conformation of C5C6 bond) the energy decreases with d. At d = 4.8 Å the energies of all three states become close to each other. At d > 4.8 Å the last two conformations become more favorable. The first of them (Fig. 4a, filled squares) has a minimum at d near 5.0–5.1 Å while the second (Fig. 4.a, filled triangles) at d = 5.1–5.2 Å. At d near 5.6 Å the energy of the first (gt) conformation drops abruptly to an energy of tg state due to hydrogen bonding inside monomer and energy of gg conformation also jumps down to energy of tg state at this distance. Thus at d > 5.7 Å we have only one combined curve for $^4C_1$ state corresponding to tg conformation.

Fig. 4b shows the dependence of two dihedral angles O5C5C6O6 and C4C5C6O6 (the same as in Fig. 2) in three sub-states of dextran monomer in chair $^4C_1$ conformation on distance between monomer ends. The three different initial pairs of these two dihedral angles (three sub-states) are: (60°, 180°) i.e. g + t conformation, (−60°,60°) i.e. g-g+ conformation, and (180°,−60°) i.e. tg- conformation. In the first stage these angles change near linearly with distance but at d near 5.5 Å these changes become more pronounced and at d = 5.6–5.7 Å abrupt transition from g + t and g-g+ conformations to tg- conformation occurs. This behavior is in agreement with drop of energy in DFT calculations for both for g + t and g-g+ states on Fig. 4a and similar drop in force at this distance on Fig. 1c (line 2) for forcefield-based simulation at T = 0 K.

We measured also the change of two dihedral angles which reflect the conformation transitions of the glucopyranose ring (same as in Fig. 3) for the same three initial conformation of C5–C6 bond in chair $^4C_1$ state (g + t, g-g and tg-) but no significant changes of these angles was observed. It means that no conformational transitions of ring itself were found in DFT simulation. But it is necessary to mention that all DFT calculations are fulfilled at zero temperature. Due to this reason some thermoactivated conformational transitions (for example chair-chair or chair-boat) can not be seen directly. But we can make conclusion about the population of different glyucopyranose conformers on the base of relative energies of different chair and boat states. Such evaluation from Fig. 4a

© 2006 WILEY-VCH Verlag GmbH & Co. KGaA, Weinheim

shows that conformation $^4C_1$ stays dominant until almost d = 6.0 Å (curves for inverted chair, boats and all other conformations have higher energies). But at d = 6.0 Å two other conformations ($^1C_4$ (open circles) and twisted boat (crosses)) have comparable energy with energy of $^4C_1$ state. It means that at this point each of these three conformations should represent near 1/3 of the whole population of the glucopyranose ring.

At higher distances d > 6.0 Å the twisted boat conformation become dominant one. Last result is in accordance with both Marszalec result obtained by MD methods and CHARMM forcefield and our Amber based MD simulations.

Conclusion

The structure and dynamical properties of the dextran under extension with constant pulling speed were calculated using Amber-Glycam04 forcefield. The main result of the present Amber-based simulation is that the plateau on the force-extension dependence can be explained by a transition of the glucopyranose rings in dextran monomers from the chair ($^4C_1$) to the inverted chair ($^1C_4$) at distances near 5.7–6.0 Å, while most of the chair to boat transition occur at higher extension.

Our previous simulation of the dextran monomer and 10mer under the constant extension force applied to dextran end is in agreement with this result.

DFT simulation of the dextran monomer under different fixed monomer length gives the results similar to that obtained by forcefield based simulation with the Amber-Glycam04 forcefield. It confirms the existence of the inverted chair ($^1C_4$) conformation at intermediate extensions (corresponding to monomer length d = 5.9–6.1 Å) and its possible important contribution in the experimental plateau region of the force-extension dependence for dextran. But further forcefield based simulations as well as ab initio calculations especially in explicit water are necessary for full understanding of polysaccharides extension.

Acknowledgements: This work was supported by EPSRC, grants GR/S67388/01 and EP/C528336/1. I.N. is thankful for partial support in framework of RFBR 05-03-32450. M.Ratner asknowledge the support by grant of NASU (Program "Nanosystems, nanomaterials and nanotechnologies", project N19/04).

[1] Reif, M.; Oesterhelt, F.; Heymann, B.; Gaub, H. E. Science **1997**. 275, 1295.
[2] Marszalek, P. E.; Oberhauser, A. F.; Pang, Y. P.; Fernandez, J. M. Nature **1998**, 396, 66.
[3] G. Lee, W. Nowak, J. Jaroniec, O. Zhang, P.E. Marszalec, Biophys. J. **2004**, 87, 1456–1465.
[4] M. Kuttel, J.W. Brady, K.J. Naidon J. Comput. Chem. **2002**, 23, 1236–1243.
[5] I.M. Neelov, D.B. Adolf, E. Paci, T.C.B. McLeish Biophys. J., **2005**, in press.
[6] S.J. Weiner, P.A. Kollman, D.T. Nguen, D.A. Case J. Comput. Chem. **1986**, 7, 230.
[7] MacKerell et al CHARMM22 J. Phys. Chem. B, **1998**, 102, 3586.
[8] M.K. Dowd, A.D. French, P.J. Reilly Carbohydrate Research, **1994**, 264, 1.
[9] H. Senderovitz, C. Parish, W.C. Still J. Am. Chem. Soc. **1996**, 118, 2078.
[10] S.W. Homans Biochemistry **1990**, 29, 9110.
[11] R.J. Woods et al J. Phys. Chem., **1995**, 99, 3832.
[12] H. Senderovitz, W.C. Still J. Org. Chem. **1997**, 62, 1427.
[13] R. Eklund, G. Widmalm Carbohydrate Research, **2003**, 338, 393.
[14] L. Hemmingsen et al Carbohydrate Research, **2004**, 339, 937.
[15] H.C. Andersen J. Chem. Phys. **1980**, 72, N4, 2384–2393.

© 2006 WILEY-VCH Verlag GmbH & Co. KGaA, Weinheim